



Assessment of performance recently developed acriflavine thin film composite nanofiltration membrane for seawater treatment and RO brine concentration

B. Garudachari*, M. Ahmed, K. A. Rajesha, J. Thomas

Kuwait Institute for Scientific Research, Water Research Center, P.O. Box: 24885, Safat 13109, Kuwait,
emails: bgarudachari@kisir.edu.kw (B. Garudachari), mahmed@kisir.edu.kw (M. Ahmed),
ralambi@kisir.edu.kw (K.A. Rajesha), jithomas@kisir.edu.kw (J. Thomas)

ABSTRACT

To enhance the permeation and salt rejection properties of polysulfone membrane, novel TiO_2 nanoparticle incorporated acriflavine thin film composite (TFC) was fabricated. Fabricated TFC membranes were characterized thoroughly using Fourier transform infra red (FT-IR), atomic force microscope, field emission scanning electron microscope and contact angle (CA). The signature peaks in FT-IR spectra were identified to confirm the interfacial polymerization (IP) of acriflavine and TMC. TiO_2 nanoparticle incorporation in the TFC layer was analysed using elemental mapping analysis and EDX. The addition of TiO_2 nanoparticle in acriflavine TFC layer resulted change in morphology of membrane and contact angle. The highest pure water flux was reached up to $67.1 \text{ Lm}^{-2} \text{ h}^{-1}$ with 0.1 weight percentage of TiO_2 nanoparticle dosage (TFC 4). The water flux of 53.0, and $44.5 \text{ Lm}^{-2} \text{ h}^{-1}$ were achieved for TFC 4 membrane using Arabian Gulf Seawater, and reverse osmosis (RO) brine, respectively. Most importantly, TFC 4 membrane showed less fouling with more than 99% of ionic rejection for magnesium, calcium, and sulfate ions. From the studies, it was concluded that, novel TiO_2 nanoparticle incorporated acriflavine TFC membranes are having high capability of rejecting divalent ions and suitable for seawater treatment and RO brine concentration applications.

Keywords: Desalination; TiO_2 nanoparticle; Salt flux; Water flux

1. Introduction

The freshwater resources in the state of Kuwait are very limited and more than 90% of freshwater is produced from thermal and membrane desalination process. The major share of seawater desalination in the state of Kuwait is taken by thermal processes which are multistage flash (MSF) and multieffect distillation. In the state of Kuwait, thermal desalination process is coupled with power generation plants to reduce the capital and operating cost. However, thermal desalination processes are suffering from scaling, corrosion, and low efficiency (low water recovery) compared with reverse osmosis (RO). In the recent decades, RO technology becoming popular as an alternative seawater desalination

technology due to high water recovery and low energy consumption compared with thermal seawater desalination. However, RO still has a number of challenges such as significant concentration polarization, scaling, and fouling (Ge et al. 2013; Stone et al. 2013; Ahmad 2012). Additionally, RO is considered as an energy-intensive system because it requires operating pressure greater than 50 atm, and the requirement of a high hydraulic pressure to overcome the osmotic pressure generated by seawater (Ge et al. 2013; Stone et al. 2013). In the recent years, thin film composite (TFC) membranes showed a promising way of producing fresh water at low-energy consumption and high purity. The selectivity, low resistance, and high flux attracted researchers to search new effective thin film coating for the

* Corresponding author.

TFC membrane fabrication process (Zh et al. 2018; Zhang et al. 2018). In membrane technology, microfiltration and ultrafiltration membranes are sources as a base polymer membrane for producing TFC membrane. The selectivity of ions in desalination process depends on the pore size, charge on the surface of membrane and hydrophilicity (Werber et al. 2016). The hydrophilicity of the membrane can be altered by incorporating nanoparticle and modification of selective layer in the thin film. Among the TFC membrane, the polyamide type cross-linking coating has attracted due to its excellent pH stability, ion selectivity, and thin film forming capability (Maruf et al. 2012). The disadvantage of polyamide-based TFC membrane is its low chlorine tolerance, less chemical stability, and low antifouling behaviour. The aforementioned drawbacks can be overcome by developing new polyamide cross-link polymer with chemically stable functional groups. Further, the modification of TFC membrane by incorporating nanoparticle showed a promising approach to overcome the chemical stability, chlorine tolerance, and antifouling characteristics (Lau et al. 2012; Son & Jegal 2010).

Acriflavine is one of the 3,6-diamine with a quaternary amine at tenth position of the anthracene ring. The diamine at the end of the anthracene ring is more basic and highly reactive. The planar structure of the acriflavine is one of the advantages for cross-link polymerization and to develop a continuous defect-free thin film (Sikorski & ski 2014; Eldaroti et al. 2013; Can et al. 2014). In the pharmaceutical field, acriflavine is generally used as an antiseptic and antibacterial agent in the drug development. In the aquarium hobby, it is used as an antifungal agent to treat various fungal infections in fish and preventing fish egg loss to fungus. The acriflavine family drugs induce cellular strain to fungus and reduce the further growth and on the other hand, acriflavine derivatives are good antibacterial and antimalarial agents (Kawai & Yamagishi 2009).

In the present study, a novel approach for the fabrication of polyamide layer is demonstrated using acriflavine as amine monomer and TMC as acid monomer via IP technique. Further, acriflavine in aqueous solution was incorporated with TiO_2 nanoparticles to study the effect of nanoparticle on permeation and selectivity of the novel TFC layer. The membranes were characterized in detail using instrumentation techniques such as atomic force microscope (AFM), field emission scanning electron microscope (FESEM) and contact angle goniometer. The practical application of TFC membranes was evaluated by performing a rejection and permeation studies for seawater sample and brine discharge obtained from the desalination plant.

2. Experimental

2.1. Preparation of acriflavine TFC membranes

Acriflavine TFC membranes were fabricated on the surface of pre-cast PSf substrate by IP method. The 0.01, 0.05, and 0.1 weight percent (wt.%) of TiO_2 nanoparticles were dispersed in two weight percentage of acriflavine aqueous solution with 1.1 equivalent of triethylamine (TEA). Clearly dispersed nanoparticle acriflavine solution was filtered to remove undissolved and agglomerated nanoparticles from the solution. The substrate membrane was clamped horizontally on the glass plate and aqueous solution of nanoparticle-dispersed acriflavine solution was poured and kept for two min to penetrate solution to pores of the substrate. The excess solution was drained off and residual drops were removed by soft rubber roller. After 1 min, 0.1% (w/v) TMC solution in hexane was added and kept for 1 min to IP, then TMC solution was drained off. The unreacted TMC was removed by hexane washing and kept inside the oven at 60°C for 10 min to complete polymerization. The newly fabricated TFC membrane was washed with deionized (DI) water and stored in DI water (Xie et al. 2012). Based on the concentration of TiO_2 used for fabricating TFC membranes, the prepared TFC membranes are labelled as TFC 1 (control: 0% TiO_2), TFC 2 (0.01% TiO_2), TFC 3 (0.05% TiO_2), TFC 4 (0.1% TiO_2). The compositions of newly fabricated TFC membranes are tabulated in Table 1. The chemical reaction involved in the formation of PA layer is shown below.

2.2. Characterization of TFC membranes

ALPHA-FTIR spectrophotometer (Bruker Company) was used to characterize the chemical structure and confirm the incorporation of TiO_2 nanoparticle in the acriflavine TFC membranes. The measurement was taken with 64 scans in the range of 4,000 to 400 cm^{-1} . The contact angles were measured using optical contact angle and interface tension meter from USA KINO (model-SL200KB). Keysight 8500 FESEM was used to study the surface and cross-sectional morphology of the membranes. The membrane surface topological features were analyzed using Concept Scientific Instrument (Nano-Observer), France, by scanning the membrane surface over $10\ \mu\text{m} \times 10\ \mu\text{m}$ dimensions.

2.3. Evaluation of membrane performance

The performance of TFC membranes was studied on self-stirred membrane permeation cell (Sterlitech HP4750 STIRRED CELL) having effective membrane diameter of

Table 1
Composition of costing solution and contact angle

SL No	Code	% Composition			Contact angle ($^\circ$)
		Acriflavine wt.%	TMC wt.%	TiO_2 wt.%	
1	TFC 1	2	0.1	0	66.89
2	TFC 2	2	0.1	0.01	53.97
3	TFC 3	2	0.1	0.05	51.89
4	TFC 4	2	0.1	0.1	51.12

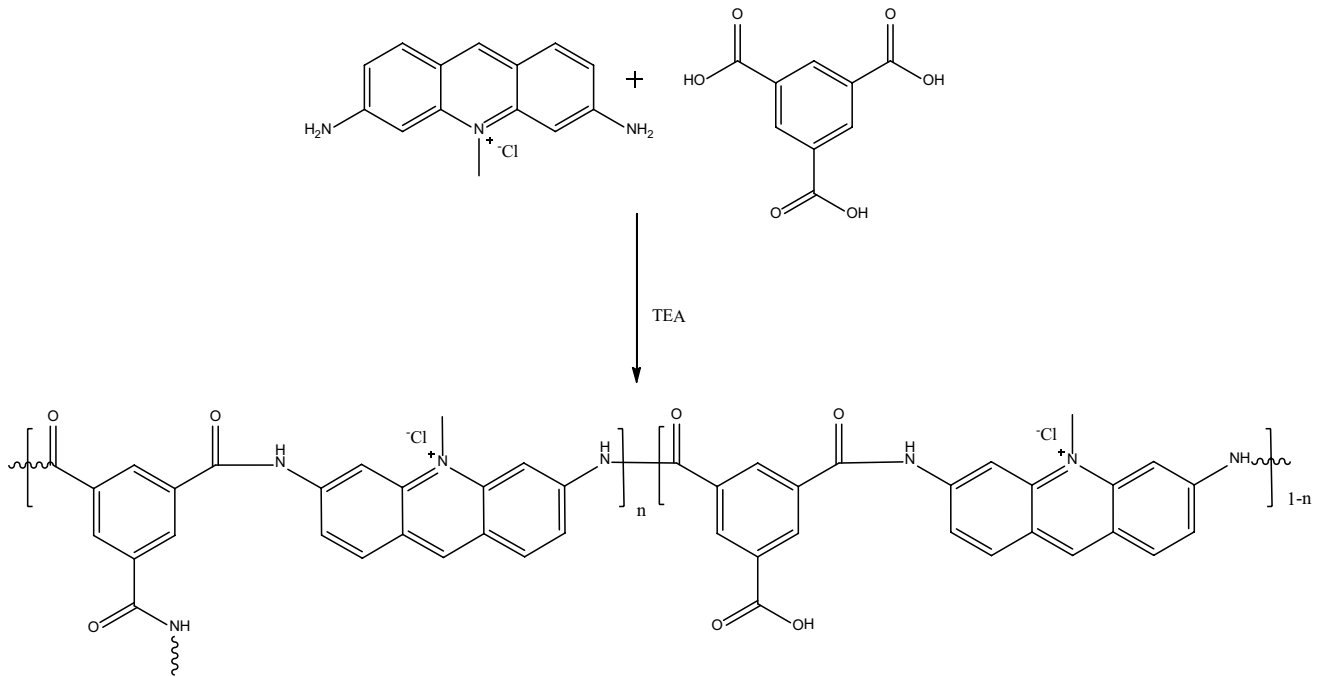


Fig. 1. Chemical reaction of acriflavine and trimesic acid (TEA: Triethylamine).

5 cm at pressure 9 bar. The feed solution used for the experiments are DI water, seawater, and RO brine. The water flux (J_w) and salt rejection (R) of the TFC membranes were calculated using Eq. (1).

$$J_w = \frac{Q}{A \times \Delta t} \quad (1)$$

where J_w (L/m² h) is the pure water flux (PWF), Q is the volume of water (L) permeated through the membrane of effective area A (m²) over a time Δt (h).

$$\% \text{ Rejection} = \left(1 - \frac{C_p}{C_f} \right) \times 100 \quad (2)$$

where C_p and C_f are the concentrations of the feed and permeate. Each membrane was tested three times and average values were reported.

3. Results and discussion

3.1. FTIR analysis

The FTIR spectra of acriflavine, PSf, TFC, and TiO₂ TFC are presented in Fig. 2. The sharp peaks at 1,457; 1,601 cm⁻¹ corresponds to C=N and C=C of the acriflavine aromatic ring, respectively. Aromatic C-H and N-methyl (N-CH₃) stretching peaks have appeared at 2,913; 2,919; 2,954; 3,030 cm⁻¹ and free amine (NH₂) as a doublet at 3,315 and 3,431 cm⁻¹. In PSf spectrum, two peaks at 1,294–1,324 cm⁻¹ correspond to O=S=O of the polysulfone and high intense peak at 1,586 cm⁻¹ is due to C=C of the aromatic rings present in the PSf polymer. The aromatic C-H and CH₃

stretching peaks have appeared at 2,873; 2,969; and 3,038 cm⁻¹ (Moradihamedani et al. 2015). In neat TFC polyamide (PA), the peak 1,445 cm⁻¹ corresponds to C=O attached to amide link (C-N) and 1,602 cm⁻¹ corresponds to the C=O of the carboxylic acid which is formed due to end of the polymer chain or end of polymer branching. The aromatic C-H and N-methyl (N-CH₃) stretching peaks have appeared at 2,987; 3,008; and 3,032 cm⁻¹. The N-H of the amide appeared as a singlet at 3,343 cm⁻¹ and disappearance of NH₂ peaks at 3,315; 3,431 cm⁻¹ and absence of 1,770 cm⁻¹ C-Cl peaks confirms the formation of PA layer (Shawky et al. 2011). The spectrum TiO₂TFC shows all the corresponding peaks of PSf, PA, and a broad peak of NH and -OH (TiO₂) at 3,389 cm⁻¹ confirms the TiO₂ incorporated acriflavine TFC.

3.2. Membrane morphology

The permeation and rejection properties of the membrane are strongly depending on the morphology of the membrane. The FESEM is the prominent technique to study the morphological variation of newly developed acriflavine TFC membrane (Hebbar et al. 2018, Khorshidi et al. 2018). Fig. 3 shows the surface, cross-sectional FESEM of TFC 4 membrane. All the membranes exhibited rigid-valley structure, which is due to the IP of acriflavine amine and TMC (Wei et al. 2011). The cross-sectional image clearly shows the formation of thin (~100–300 nm) PA layer on the PSf substrate membrane. In the cross-section of the substrate membrane, the figure-type interconnected structure which will provide little resistance to permeate transportation and mechanical strength. On the top of the figure-type projection, a distinctive very thin sublayer of PA confirms the formation of active TFC layer which is responsible for the selectivity of ions as well as flux (Lau et al. 2015; Lalia et al. 2013).

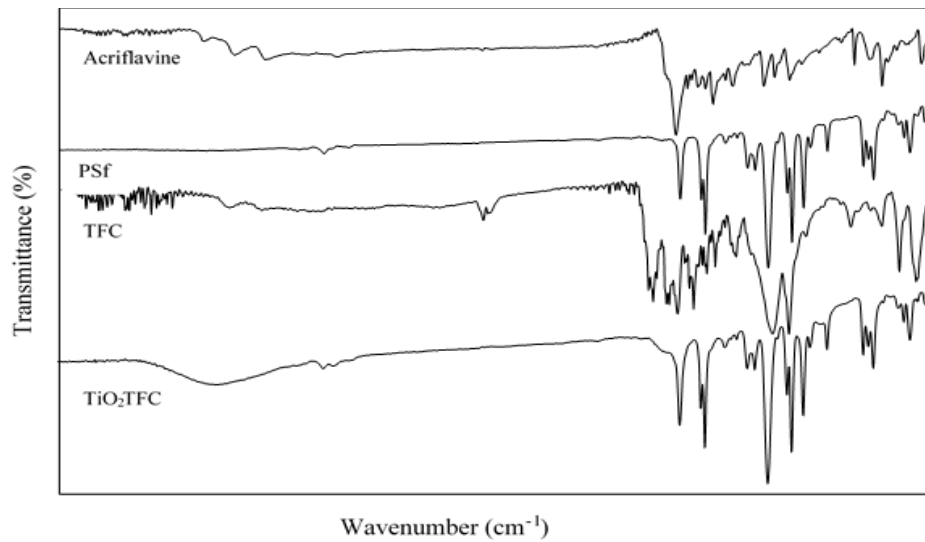


Fig. 2. FT-IR spectra of acriflavine, PSf, TFC, and TiO₂/TFC.

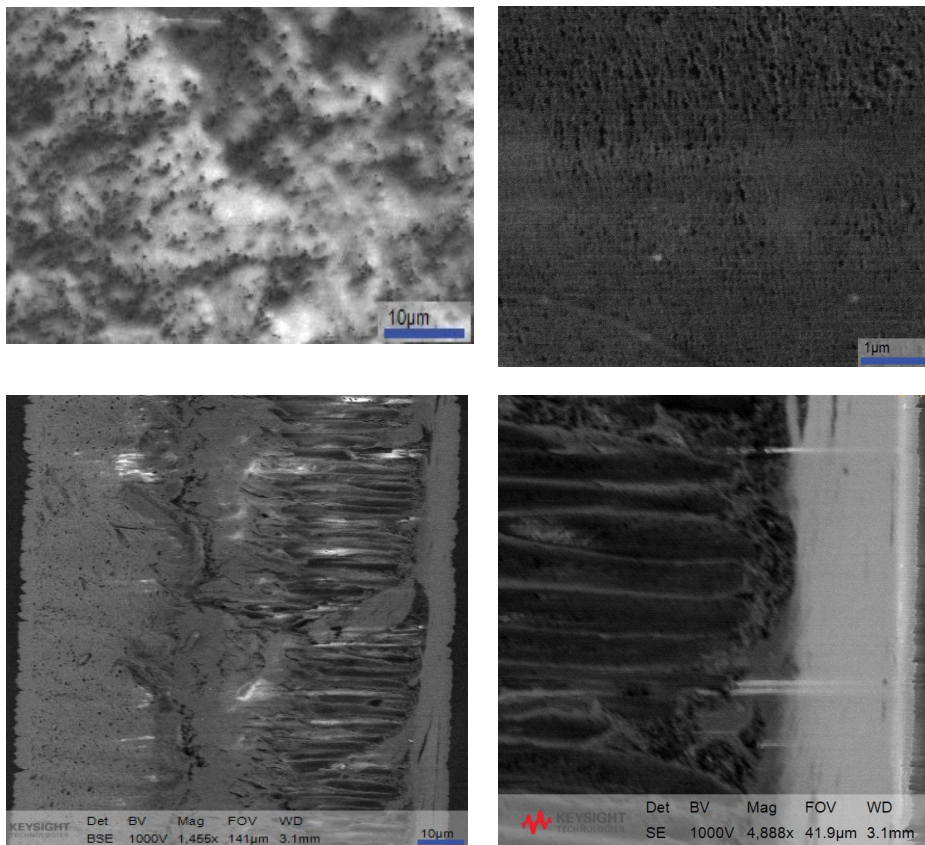


Fig. 3. Magnified surface, cross-sectional FESEM images of TFC 4.

The surface analysis was carried out to study the topological feature and surface roughness of acriflavine TFC membranes using nano-observer AFM instrument by scanning the membrane surface over $10 \mu\text{m} \times 10 \mu\text{m}$ dimensions. The three-dimensional AFM images are shown in Fig. 4 and surface roughness parameters are presented

in Table 2 as maximum mean roughness (R_a), route mean square roughness (R_q) and maximum feature height (R_{max}). From the results, increasing trend of roughness values by increasing the TiO₂ concentration in the acriflavine TFC membrane was observed. The lowest maximum mean roughness (R_a) observed was 19.2 nm for acriflavine TFC

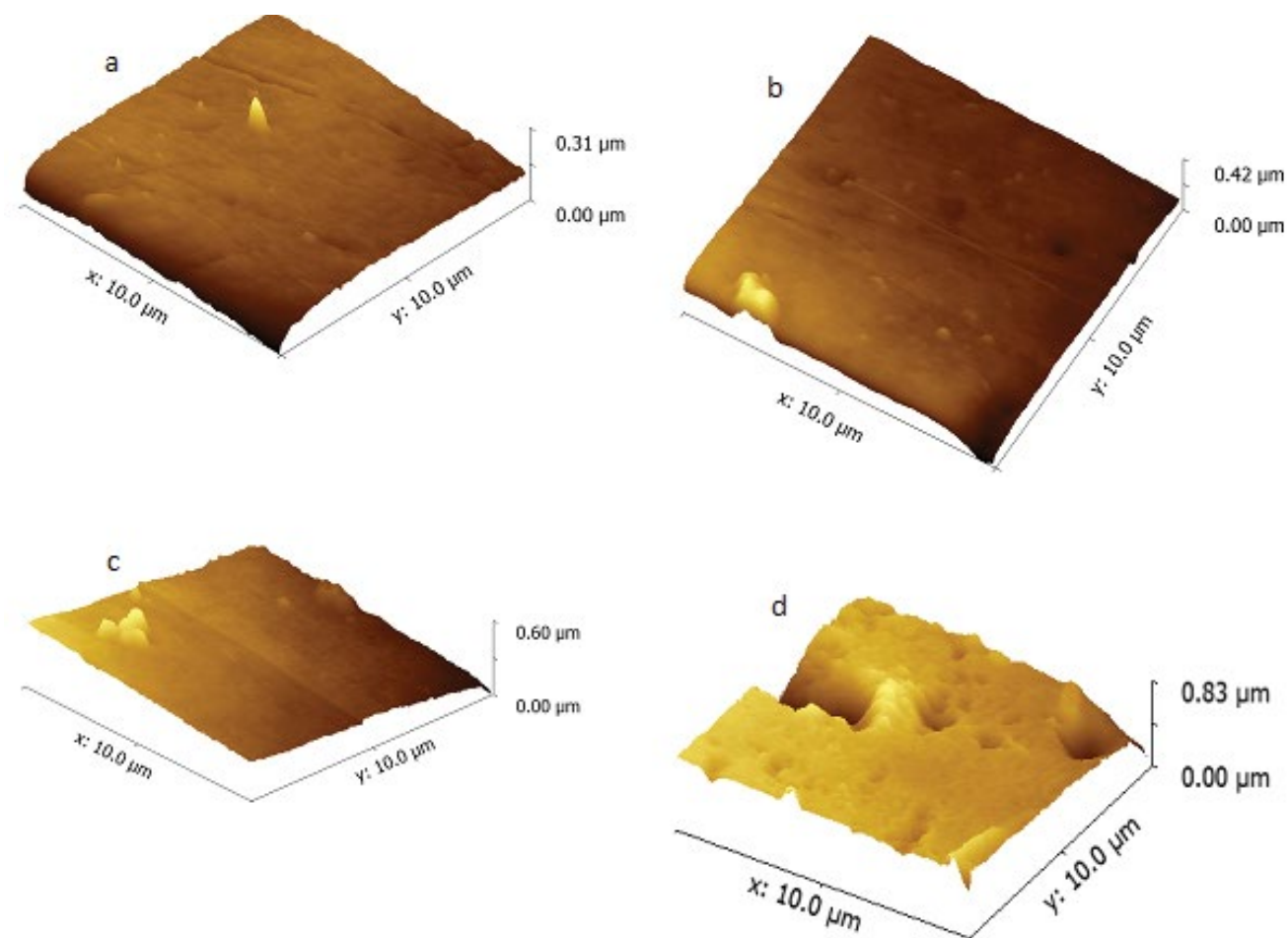


Fig. 4. Three-dimensional AFM images of (a) TFC 1, (b) TFC 2, TFC 3 and (c) TFC 4.

membrane without any nanoparticle addition and highest was observed for TFC 4 (71.7 nm). It is interesting to note that the roughness of the membrane increases as the concentration of TiO_2 increases in acriflavine TFC. This may be due to participation/interaction of TiO_2 nanoparticles in the process of the IP reaction and also fast reaction rate between acriflavine, TMC in the presence of TiO_2 nanoparticles (Ghanbari et al. 2015).

3.3. Contact angle study

The membrane hydrophilicity is a very important parameter for high water flux and antifouling property. The change in hydrophilicity (CA) with the addition of TiO_2 nanoparticle was investigated by measuring contact angle. In general, lower is the CA of the membrane indicates the more hydrophilic nature (Hebbar et al. 2015). From Table 1, highest CA (66.89°) was observed for acriflavine neat TFC membrane compared with TiO_2 nanoparticle incorporated membranes. The TFC 1 (neat TFC) having N-CH_3 group in the acriflavine aromatic ring may be the reason for the highest CA. The CA of the acriflavine TFC membrane was decreased with the loading of 0.01 to 0.05, 0.1 percentage of TiO_2 , this is due to the additional porous structure on PA

Table 2
Surface roughness parameters of membranes

Membrane	Roughness		
	R_a (nm)	R_q (nm)	R_{max} (nm)
TFC 1	19.2	24.5	163.3
TFC 2	37.1	47.4	170.1
TFC 3	69.9	86.2	324.5
TFC 4	71.7	104.9	593.6

and both chemical and structural properties of the membrane surface (Peyravi et al. 2014).

3.4. Membrane performance study

The desalination performance of the TFC membrane mainly depends on the structural properties of thin film and its chemical nature. However, nature of feed solution also plays a major role. Preliminary permeation test was conducted for all the membrane using DI water as feed. From the results (Fig. 5), it is clearly shown that the acriflavine TFC membrane with 0.1% TiO_2 showed high pure water

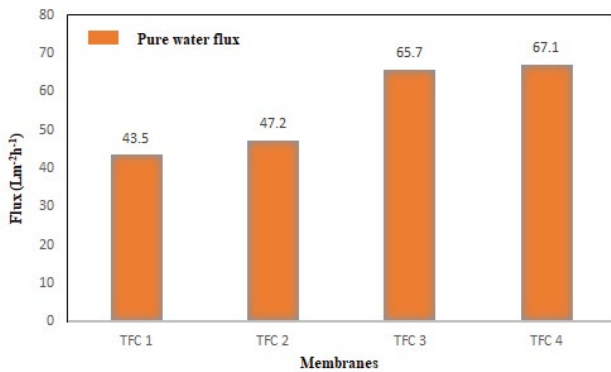


Fig. 5. Pure water flux of the membranes at 0.9 MPa pressure.

flux compared with other membranes. The order of pure water flux is TFC 4 > TFC 3 > TFC 2 > TFC 1. This increasing trend of pure water flux with increasing concentration of TiO₂ in acriflavine TFC is due to the additional porous structure of PA and both chemical and structural properties of the membrane surface. On the other hand, the charge on the PA layer due to the quaternary amine (positive charge in the acriflavine aromatic ring: ⁺N-CH₃) will attract the water molecules on the surface of the membrane will lead to enhanced permeation.

The actual seawater desalination study was conducted for TFC 4 membrane using Arabian Gulf seawater (AGS) and RO brine as a feed. Table 3 shows the physicochemical analysis of AGS and RO brine. The desalination performance of the TFC 4 membrane for AGS and RO brine was shown in Fig. 6 and flux obtained was 53.0 and 44.5 Lm⁻²h⁻¹ for AGS and RO brine, respectively. The physicochemical parameters of permeate water from the desalination of AGS and RO brine was shown in Table 4 and percentage of salt rejection are presented in Fig. 7. The permeate flux for RO brine feed is less compared with AGS, this may be due to the high salinity of RO brine. TFC 4 membrane showed significant high rejections for divalent ions compared with

Table 3
Physicochemical analysis of AGS and RO brine

Parameters/unit	AGS at Doha desalination plant Kuwait	RO brine
Total dissolved solids, mg/L	45,377	54,900
Conductivity	58.3	69.4
Magnesium, mg/L	1,325	1,673
Calcium, mg/L	730	1,090
Boron, mg/L	3.7	9.8
Lithium, mg/L	1.21	1.7
Strontium, mg/L	14.6	121
Sodium, mg/L	14,488	17,905
Potassium, mg/L	316.4	997
Chloride, mg/L	24,876	68,593
Sulfate, mg/L	3,430.5	4,159

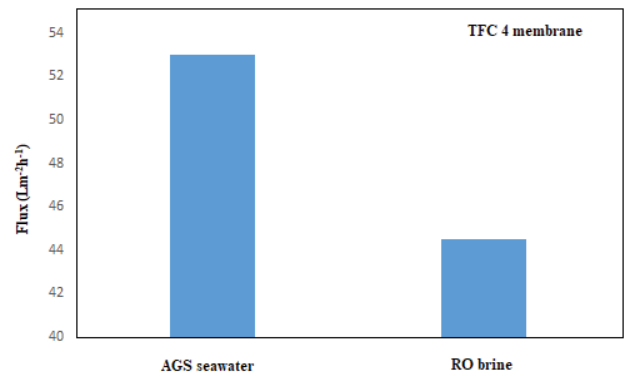


Fig. 6. Water flux of the TFC 4 membrane at 0.9 MPa pressure for AGS and RO brine feed.

Table 4
Physicochemical parameters of permeate water from the desalination of AGS and RO brine

Parameters/unit	Permeate		Reject	
	AGS	RO brine	AGS	RO brine
Conductivity	27.05	71.09	62.856	85.11
Magnesium, mg/L	5.8	197	2,039	3,013
Calcium, mg/L	6.0	407.2	1,006	1,507
Sodium, mg/L	12,051	12,051	13,316	30,520
Potassium, mg/L	100	688	340	1,223
Chloride, mg/L	20,230	41,176	26,086	68,603
Sulfate, mg/L	3.9	6.84	6,433	21,704

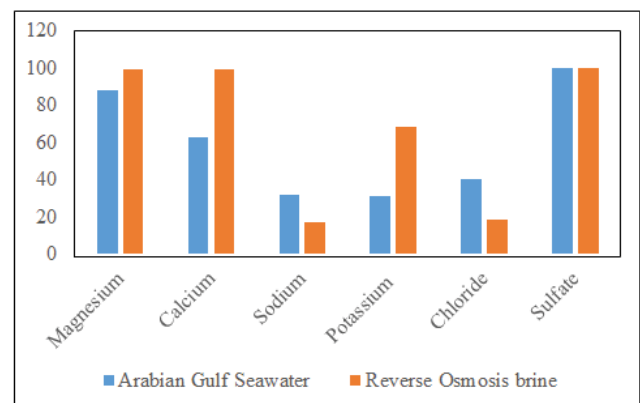


Fig. 7. Percentage salt rejection.

monovalent ions for AGS and RO brine feed. The reason for highest rejection for divalent ions is due to the larger size, higher charge of ions (Krieg et al. 2004). The rejected ions are 88.2 (Mg²⁺), 62.6 (Ca²⁺), 99.8 (SO₄²⁻), 39.8 (Cl⁻), 31.8 (Na⁺), and 30.9 (K⁺) percentage for AGS as a feed and 99.5 (Mg²⁺), 99.1 (Ca²⁺), 99.8 (SO₄²⁻), 68.3 (K⁺), 18.6 (Cl⁻), and 16.8 (Na⁺) percentage for RO brine as a feed. TFC 4 membrane rejected 99% of Mg²⁺, Ca²⁺, and SO₄²⁻. The permeate obtained from

the desalination experiments shows very low concentrations of divalent salts. But the monovalent salts rejection is low as compared with divalent ions. Based on the salt rejection study, acriflavine TFC membrane is a highly promising membrane for seawater desalination pretreatment application and RO brine concentration. The long-term experimental (24 h test) test shows less fouling for TFC 4 membrane compared with TFC 1 membrane for RO brine as a feed. The antifouling character of TFC 4 membrane may be due to neutralized charge distribution on the acriflavine TFC with TiO₂ nanoparticle on the surface of membrane and change in surface morphology of membrane.

4. Conclusion

The TiO₂ nanoparticle incorporated acriflavine TFC membranes were fabricated on PSf support by an IP method. The fabricated novel TFC membranes were characterized using FT-IR, AFM, and SEM. The FT-IR spectra show the TiO₂ nanoparticle incorporation in acriflavine TFC and cross-sectional SEM and 3D AFM images exhibited the changes in morphology and surface roughness properties of resultant acriflavine TFC membrane. The inclusion of TiO₂ nanoparticle into acriflavine TFC membrane aided as performance modifier which increased water flux and high salt rejection. The TFC 4 membrane showed contact angle of 51.12° and pure water flux of 67.1 Lm⁻²h⁻¹. The salt rejection experiments showed excellent rejection for divalent ions for AGS and RO brine feed solution. The study concluded that TiO₂ nanoparticle incorporated acriflavine TFC membranes are having the high capability of rejecting divalent ions and suitable in desalination pretreatment and RO brine concentration applications.

Acknowledgements

The authors are thankful to the Kuwait Institute for Scientific Research (KISR) for funding and supporting the implementation of this research work.

References

- Ahmad, M., and Williams, P., 2011, "Assessment of desalination technologies for high saline brine applications - Discussion Paper". *Desalination*, 30: 22–36.
- Ahmad, M., 2012, "Assessment of Freeing Desalination Technologies". Ph.D. Thesis, Swansea University, UK.
- Baker, R. W., 2012, "Membrane Technology and Applications". Third Edition. Membrane Technology and Research, Inc. Menlo Park, California, 1–538.
- Butler, D., 2017, "Global Challenges: Water". *Global Challenges* 1: 61–62.
- Can, H. K., Karakus, G., and Tuzcu, N., 2014, "Synthesis, characterization and in vitro antibacterial assessments of a novel modified poly[maleic anhydride-alt-acrylic acid]/acriflavine conjugate". *Polymer Bulletin*, 71: 2903–2921.
- Eldaroti, H. H., Gadir, S. A., Refat, M. S., and Adam, A. M. A., 2013, "Charge Transfer Complexes of the Donor Acriflavine and the Acceptors Quinol, Picric acid, TCNQ and DDQ: Synthesis, Spectroscopic Characterizations and Antimicrobial Studies". *International Journal of Electrochemical Science*, 8: 5774 – 5800.
- Ge, Q., Ling, M., and Chung T. S., 2013, "Draw Solutions for Forward Osmosis Processes: Developments, Challenges, and Prospects for Future". *Journal of Membrane Science*, 442: 225–237.
- Ghanbari, M., Emadzadeh, D., Lau, W. J., Matsuura, T., and Ismail, A. F., 2015, "Synthesis and characterization of novel thin film nanocomposite reverse osmosis membranes with improved organic fouling properties for water desalination". *RSC Advances*, 5: 21268–21276.
- Hebbbar, R. S., Isloor, A. M., Ismail, A., Shilton, S. J., Obaid, A., and Fun, H.-K., 2015, "Probing the morphology and anti-organic fouling behaviour of a polyetherimide membrane modified with hydrophilic organic acids as additives". *New Journal of Chemistry*, 39: 6141–6150.
- Hebbbar, R. S., Isloor, A. M., Prabhu, B., Asiri, I. A. M., and Ismail, A. F., 2018, "Removal of metal ions and humic acids through polyetherimide membrane with grafted bentonite clay". *Scientific Reports*, 8: DOI:10.1038/s41598-018-22837-1.
- Kawai, M., and Yamagishi, J., 2009, "Mechanisms of action of acriflavine: electron microscopic study of cell wall changes induced in *Staphylococcus aureus* by acriflavine". *Microbiology and Immunology*, 53: 481–486.
- Khorshidi, B., Biswas, I., Ghosh, T., Thundat, T., and Sadrzadeh, M., 2018, "Robust fabrication of thin film polyamide-TiO₂ nanocomposite membranes with enhanced thermal stability and anti-biofouling propensity". *Scientific Reports*, 8: DOI:10.1038/s41598-017-18724-w.
- Krieg, H. M., Modise, S. J., Keizer, K., and Neomagus, H. W. J. P., 2004, "Salt rejection in nanofiltration for single and binary salt mixtures in view of sulphate removal". *Desalination*, 171: 205–215.
- Lalia, B. S., Kochkodan, V., Hashaiekeh, R., and Hilal, N., 2013, "A review on membrane fabrication: Structure, properties and performance relationship". *Desalination*, 326: 77–95.
- Lau, W. J., Ismail, A. F., Goh, P. S., Hilal, N., and Ooi, B. S., 2015, "Characterization Methods of Thin Film Composite Nanofiltration Membranes". *Separation & Purification Reviews*, 44: 135–156.
- Lau, W. J., Ismail, A. F., Misdan, N., and Kassim, M. A., 2012, "A recent progress in thin film composite membrane: A review". *Desalination*, 287: 190–199.
- Maruf, S. H., Ahn, D. U., Pellegrino, J., Killgore, J. P., Greenberg, A. R., and Ding, Y., 2012, "Correlation between barrier layer Tg and a thin-film composite polyamidemembrane's performance: Effect of chlorine treatment". *Journal of Membrane Science*, 405–406: 167–175.
- Mohanty, K., and Purkait, M. K., 2011, "Membrane Technologies and Applications". CRC Press Book Taylor & Francis Group, ISBN9781439805268.
- Moradihamedani, P., Ibrahim, N. A., Yunus, W. M. Z. W., and Yusof, N. A., 2014, "Study of Morphology and Gas Separation Properties of Polysulfone/Titanium Dioxide Mixed Matrix Membranes". *Polymer Engineering and Science*, DOI 10.1002/pen.23887.
- OECD., 2008, "The organization for economic co-operation and development. OECD, environmental Outlook to 2030". OECD Publishing, 1–13.
- Peyravi, M., Jahanshahi, M., Rahimpour, A., Javadi, A., and Hajavi, S., 2014, "Novel thin film nanocomposite membranes incorporated with functionalized TiO₂ nanoparticles for organic solvent nanofiltration". *Chemical Engineering Journal*, 241: 155–166.
- Shawky, H. A., Chae, S.-R., Lin, S., and Mark, R., 2011, "Wiesner. Synthesis and characterization of a carbon nanotube/polymer nanocomposite membrane for water treatment". *Desalination*, 272: 46–50.
- Sikorski, A., and ski, D. T., 2014, "Synthesis and structural characterization of a cocrystal salt containing acriflavine and 3,5-dinitrobenzoic acid". *Tetrahedron Letters*, 55: 2253–2255.
- Son, S. H., and Jegal, J., 2011, "Preparation and characterization of polyamide reverse-osmosis membranes with good chlorine tolerance". *Journal of Applied Polymer Science*, 120, 1245–1252.
- Stone, M. L., Rae, C., Stewart, F. F., and Wilson, A. D., 2013, "Switchable Polarity Solvents as Draw Solute for Forward Osmosis". *Desalination*, 312: 124–129.
- Tabe-Mohamadi, A., 2007, "A Review of the Applications of Membrane Separation Technology in Natural Gas Treatment". *Separation Science and Technology*, 34: 2095–2111.
- Wei, J., Qiu, C., Tang, C. Y., Wang, R., and Fane, A. G., 2011, "Synthesis and characterization of flat-sheet thin film composite

- forward osmosis membranes". *Journal of Membrane Science*, 372: 292–302.
- Werber, J. R., Deshmukh, A., and Elimelech, M., 2016, "The Critical Need for Increased Selectivity, Not Increased Water Permeability, for Desalination Membranes". *Environmental Science & Technology Letters*, 3: 112–120.
- Xie, W., Geise, G. M., Freeman, B. D., Lee, H-S., Byun, G., and McGrath, J. E., 2012, "Polyamide interfacial composite membranes prepared from m-phenylene diamine, trimesoyl chloride and a new disulfonated diamine". *Journal of Membrane Science*, 403–404: 152–161.
- Youssef, P. G., AL-Dadah, R. K., and Mahmoud, S. M., 2014, "Comparative Analysis of Desalination Technologies". *Energy Procedia*, 61: 2604–2607.
- Zh, J., Yuan, S., Uliana, A., Hou, J., Li, J., Li, X., Tian, M., Chen, Y., Volodin, A., and Bruggen, B. V. D., 2018, "High-flux thin film composite membranes for nanofiltration mediated by a rapid co-deposition of polydopamine/piperazine". *Journal of Membrane Science*, doi.org/10.1016/j.memsci.2018.03.004.
- Zhang, H-L., Gao, Y-B., and Gai, J., 2018, "Guanidinium-Functionalized Nanofiltration Membranes Integrating Anti-fouling and Antimicrobial Effect". *Journal of Materials Chemistry A*, DOI:10.1039/C8TA00342D.